ISBN: 978-3-95450-231-8 ISSN: 2673-5490 doi: 10.18429/JACoW-IPAC2023-WEPA054

BEAM DYNAMICS STUDY OF A CW L-BAND SRF GUN FOR THE HIGH DUTY CYCLE EUXFEL

E. Gjonaj*, Technische Universität Darmstadt, Darmstadt, Germany
D. Bazyl, Deutsches Elektronen-Synchrotron, Hamburg, Germany

Abstract

The upgrade of the European XFEL (EuXFEL) to support a high duty cycle (HDC) operation mode requires new design concepts for the electron gun. Among other variants, a 1.6-cell TESLA-type RF gun is preferred. This design employs an unconventional emittance compensation scheme. It provides embedded RF focusing by means of a retracted cathode geometry. Such a scheme has been previously tested, e.g., at the ELBE accelerator of the HZDR. However, the beam dynamics characterization of the gun remains a challenge. In this work, we present analytical estimations for the RF compensation scheme as well as beam dynamics simulation and optimization studies for the new gun design in the parameter range of the EuXFEL.

INTRODUCTION

A high gradient L-band superconducting RF gun has been proposed for the future upgrade of the EuXFEL to support continuous wave operation with up to 100% duty-cycle [1]. The gun consists of a 1.6-cell TESLA-type cavity made of bulk Nb (see Fig. 1) providing a TM_{010}-accelerating mode at 1.3 GHz (cf. [2]). A crucial feature of the gun is that the cathode is inserted via an adjustable cathode plug. The gap forming between the retracted cathode and the cavity backwall acts as a lens, with the radial component of the RF field compensating for the space-charge forces during bunch emission. For this reason, this design has been presented before as a possible emittance compensation scheme [3]. In this paper, we investigate the effectiveness of this scheme for the SRF gun designated for the EuXFEL HDC-upgrade.

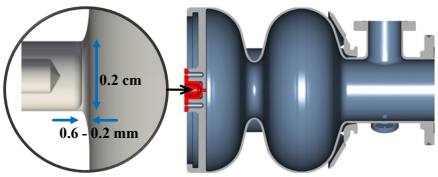

Figure 1: Geometry of the SRF gun with adjustable cathode including details of the cathode plug structure.

A consequence of a this gun design is that the accelerating field at the cathode is reduced. Figure 2 shows the accelerating field on-axis in the vicinity of the cathode. While this field is nearly constant for a flat-wall gun, its magnitude at the cathode drops by about 25% for a cathode retraction of 0.6 mm. Throughout the paper, the peak RF field magnitude in the gun is fixed to 50 MV/m.

* gjonaj@temf.tu-darmstadt.de

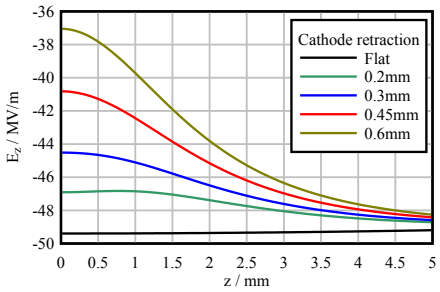

Figure 2: Accelerating field in the cathode region for different cathode retractions.

ANALYSIS

In order to quantify the balance of transverse forces during bunch emission we consider the simple situation depicted in Fig. 3. It shows a uniformly charged cylindrical bunch at an arbitrary instant in time as it is emitted out of the cathode. The radius of the bunch is a, whereas its final length when the emission process is completed is L_0. The line charge density is, therefore, constant $\lambda_0 = Q/L_0$, where Q is the final charge of the bunch. For simplicity, we consider RF focusing and space-charge fields at different radial positions, however, always at the bunch center $z = L/2$, where $L \leq L_0$ is the instantaneous bunch length. To complete the setting, we must consider the contribution of image charges at the cathode, in addition the self-field of the bunch.

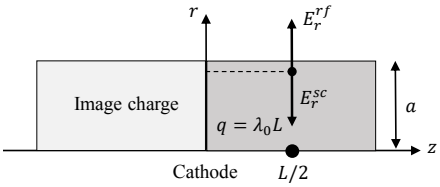

Figure 3: Uniform cylindrical bunch at an arbitrary time instant before the emission process is completed.

RF Focusing

The transverse component of the RF field to first order expansion in r is given by,

$$E_r^{rf}(r,z,t) = -\frac{\partial E_z^{rf}(z,t)}{\partial z} r, \qquad (1)$$

where $E_z^{rf}(z,t)$ is the accelerating field on-axis. We assume that all particles in the bunch "see" the same RF phase corresponding to maximum acceleration at $t = 0$. Thus, the proportionality factor in Eq. (1) can be directly computed from the derivative of the accelerating field at this

ISBN: 978-3-95450-231-8 ISSN: 2673-5490 doi: 10.18429/JACoW-IPAC2023-WEPA054

time. This factor uniquely determines the electric field strength in the radial direction. We may, therefore, define the *focusing strength* of the RF field at the bunch center as $F_r^{rf}(L) = -\partial E_z^{rf}(r,z,0)/\partial z|_{z=L/2}$. Figure 4 depicts the RF focusing strength for different bunch lengths L using the accelerating fields in Fig. 2. In the figure, a final bunch length of $L_0 = 2\,\mathrm{mm}$ is assumed. Obviously, this factor is close to zero for a flat-wall gun (not shown in the figure) and increases with increasing cathode retraction.

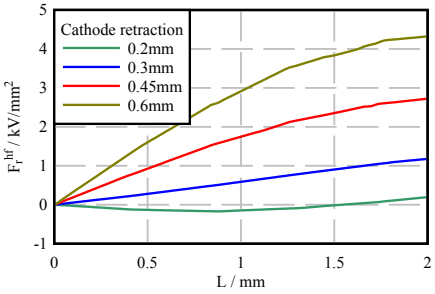

Figure 4: Rf focusing strength at the center of the bunch for different bunch lengths and cathode retractions.

Space-Charge Defocusing

Assuming that the bunch close to the cathode is non-relativistic, the radial space-charge field component is [4]:

$$E_r^{sc}(r,\Delta z) = \frac{\lambda_0}{2\pi^2\varepsilon_0}\int_0^\pi d\phi\cos\phi\log\left(\frac{R_- - z_-}{R_+ - z_+}\right), \quad (2)$$

where $\Delta z = z - L/2$ is the relative position with respect to the bunch center, $z_\pm = \Delta z \pm L/2$ and $R_\pm = \sqrt{r^2 + a^2 - 2ra\cos\phi + z_\pm^2}$. This expression can be integrated numerically including the image charge contribution. The resulting space-charge field is not strictly linear in r. However, it is so when the aspect ratio of the bunch, L/a becomes large. For the considered distributions, this condition is fulfilled almost everywhere, except for shortly after emission starts where $L \ll L_0$. Thus, we may describe the net effect of the space-charge field at the bunch center by the *defocusing strength*, $F_r^{sc}(r,L) = E_r^{sc}(r,0)/r$.

The space-charge defocusing for a 100 pC bunch of typical rms-size, $\sigma_r = 2a$, of 0.16 mm and a final length of $L_0 = 2\,\mathrm{mm}$ is depicted in Fig. 5. In order to emphasize the nonlinearity of space-charge fields, the defocusing factor is computed close to the bunch center and at its edge, respectively. These curves converge when the bunch length becomes large, while a certain deviation is observed for the short bunch lengths in the initial emission stage.

Comparing Figs. 4 and 5, it becomes clear that the RF focusing cannot fully compensate for the space-charge field of the bunch. For the largest retraction of 0.6 mm and a fully developed bunch, the RF focusing accounts for about half of the space-charge defocusing effect. Note that this description neglects the longitudinal beam dynamics as well as magnetic field contributions. Furthermore, the accelerating field at

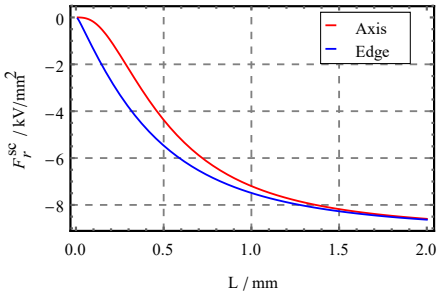

Figure 5: Space-charge defocusing on-axis and at the edge of the bunch, respectively, vs. bunch length at the cathode.

the cathode is lower for a retracted cathode compared to the flat-wall case (cf. Fig. 2) so that the time spent by the bunch in the space charge dominated cathode region is longer. Therefore, the above estimations likely overestimate the RF-compensation effect.

Beam Dynamics in the Gun

In the following, we consider the actual beam dynamics of a 100 pC bunch with nominal parameters taken from [5]. A radial laser pulse with $\sigma_r = 0.16\,\mathrm{mm}$ and a Gaussian profile with $\sigma_t = 7.3\,\mathrm{ps}$ is applied at the cathode. Magnetic focusing is provided by a solenoid with $B_{z\max} = 0.184\,\mathrm{T}$. All simulations are performed with the 3D tracking code REPTIL [6] using 400k macroparticles.

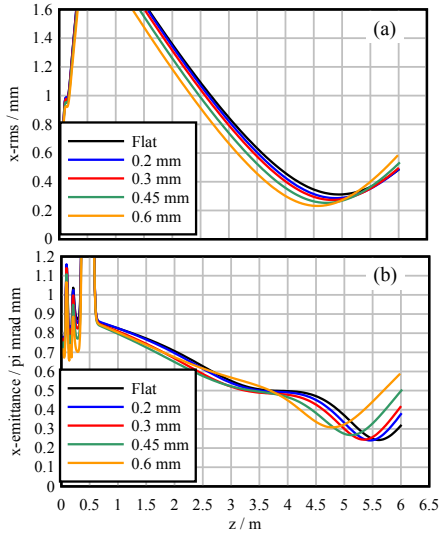

Figure 6: Bunch size (a) and transverse emittance (b) along the beam line for different cathode retractions.

The results for the bunch size and its transverse emittance up to a distance of 6 m from the cathode are shown in Fig. 6. There is a clear impact of the cathode plug retraction. However, the results are difficult to interpret. The minimum bunch size decreases with cathode retraction owing to the RF focusing at the cathode. However, the more interesting minimum emittance does the opposite. In addition, the position of emittance minimum is shifted by nearly 1 m to the

ISBN: 978-3-95450-231-8 ISSN: 2673-5490 doi: 10.18429/JACoW-IPAC2023-WEPA054

left. This indicates that the optimal working point of the gun might be different for every cathode position and, thus, it needs to be determined separately.

GUN OPTIMIZATION

To obtain the optimal parameters for each cathode retraction, we apply a genetic optimization procedure based on the NSGA-II algorithm [7] in combination with REPTIL simulations. In each optimization step, we vary the laser spot size and its pulse duration, the solenoid strength, the solenoid position and the RF phase of the gun relative to the maximum acceleration phase. It turns out, that a single-objective optimization using the minimum transverse emittance as objective function is sufficient to obtain conclusive results. In the optimization procedure, the population size was set to 64 and the number of generations to 50.

Figure 7 shows the optimized transverse emittances for each retracted cathode position. Note that the first point in the graph corresponds to the case of a conventional flat-wall gun rather than to zero-retraction in the gun design with a cathode plug. An emittance compensation effect is clearly observed for increasing amounts of cathode retraction. Thereby, a sharp emittance minimum is obtained for a retraction of 0.45 mm. For larger retractions, the emittance quickly deteriorates, presumably, due to the strongly reduced acceleration at the cathode.

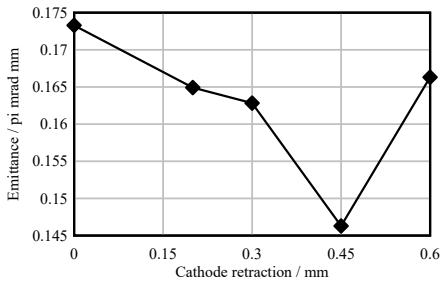

Figure 7: Optimized emittances vs. cathode retraction.

The RF compensation scheme lowers the optimum emittance by at most ~ 20%, which is expected from the previous analysis. In all cases, however, the new gun design does not lead to emittance deterioration, when the gun parameters are chosen carefully. A summary of the optimal gun parameters for different cathode retractions is listed in Table 1. The main difference to the case of a flat-wall gun is the longer pulse length and the position of the solenoid (Z_B), which must be adjusted for a retracted cathode design.

Figure 8 depicts the progressions of the beam size, core emittance and uncorrelated energy spread along the beam line for a cathode retraction of 0.45 mm and for a flat-wall gun at the respective optimal working points. All these quantities are improved in the new gun design. In particular, the core emittance is reduced to almost the thermal emittance of the cathode, thus, showing that the emittance compensation scheme is effective.

Table 1: Optimized Gun Parameters (Δ is the Retraction)

Δ(mm)	σ_r(mm)	σ_t(ps)	B(T)	Z_B(m)	ϕ_{rf}(°)
Flat	0.107	10	0.18	0.46	1.33
0.2	0.089	12.5	0.18	0.46	1.76
0.3	0.098	12.4	0.18	0.46	1.55
0.45	0.108	12.7	0.17	0.52	1.28
0.6	0.116	13.6	0.18	0.46	1.7

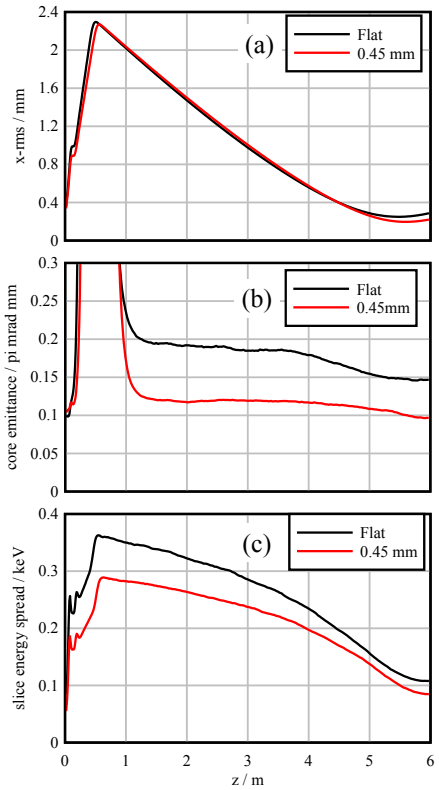

Figure 8: Beam size (a), core emittance (b) and slice energy spread (c) along the gun beam line for a cathode retraction of 0.45 mm compared to a flat-wall gun.

CONCLUSION

The analysis in the paper shows that the emittance compensation scheme based on an RF gun design with retracted cathode is effective. The effect of cathode retraction is, however, comparatively small. It furthermore, depends on the gun parameters and, naturally, on the bunch charge. For the SRF gun designated for the EuXFEL HDC-upgrade and a 100 pC bunch, we find the optimum emittance to be by up to 20% lower than for a conventional flat-wall gun. In all cases, the beam quality does not deteriorate when the operation parameters of the gun are properly chosen.

REFERENCES

[1] H. J. Qian and E. Vogel, "Overview of CW RF Guns for Short Wavelength FELs", in *Proc. FEL'19*, Hamburg, Germany, Aug. 2019, pp. 290–296. doi:10.18429/JACoW-FEL2019-WEA01

ISBN: 978-3-95450-231-8 ISSN: 2673-5490 doi: 10.18429/JACoW-IPAC2023-WEPA054

[2] "Status of the All Superconducting Gun Cavity at DESY", in *Proc. SRF'19*, Dresden, Germany, Jun.-Jul. 2019, pp. 1087–1090. doi:10.18429/JACoW-SRF2019-THP080

[3] H. Vennekate *at al.*, "Emittance compensation schemes for a superconducting rf injector", *Phys. Rev. Accel. Beams*, vol. 21, no. 9, p. 093403, Sep. 2018. doi:10.1103/PhysRevAccelBeams.21.093403

[4] K.J. Kim, "Rf and space-charge effects in laser-driven rf electron guns", *Nucl. Instrum. Methods Phys. Res. Sect. A*, vol. 275, no. 2, pp. 201–218. Feb. 1989. doi:10.1016/0168-9002(89)90688-8

[5] D. Bazyl *et al.*, "CW Operation of the European XFEL: SC-Gun Injector Optimization, S2E Calculations and SASE Performance", 2021. doi:10.48550/arXiv.2111.01756

[6] E. Gjonaj, "REPTIL – Status of development and overview of capabilities", DESY, 2022, https://www.desy.de/xfel-beam/s2e/talks/2022_01_11/EG.pdf

[7] K. Deb *et al.*, "A Fast and Elitist Multiobjective Genetic Algorithm: NSGA-II", *IEEE Trans. Evol. Comp.*, vol. 6, no. 2, pp. 182–197, Apr. 2002. doi:10.1109/4235.996017